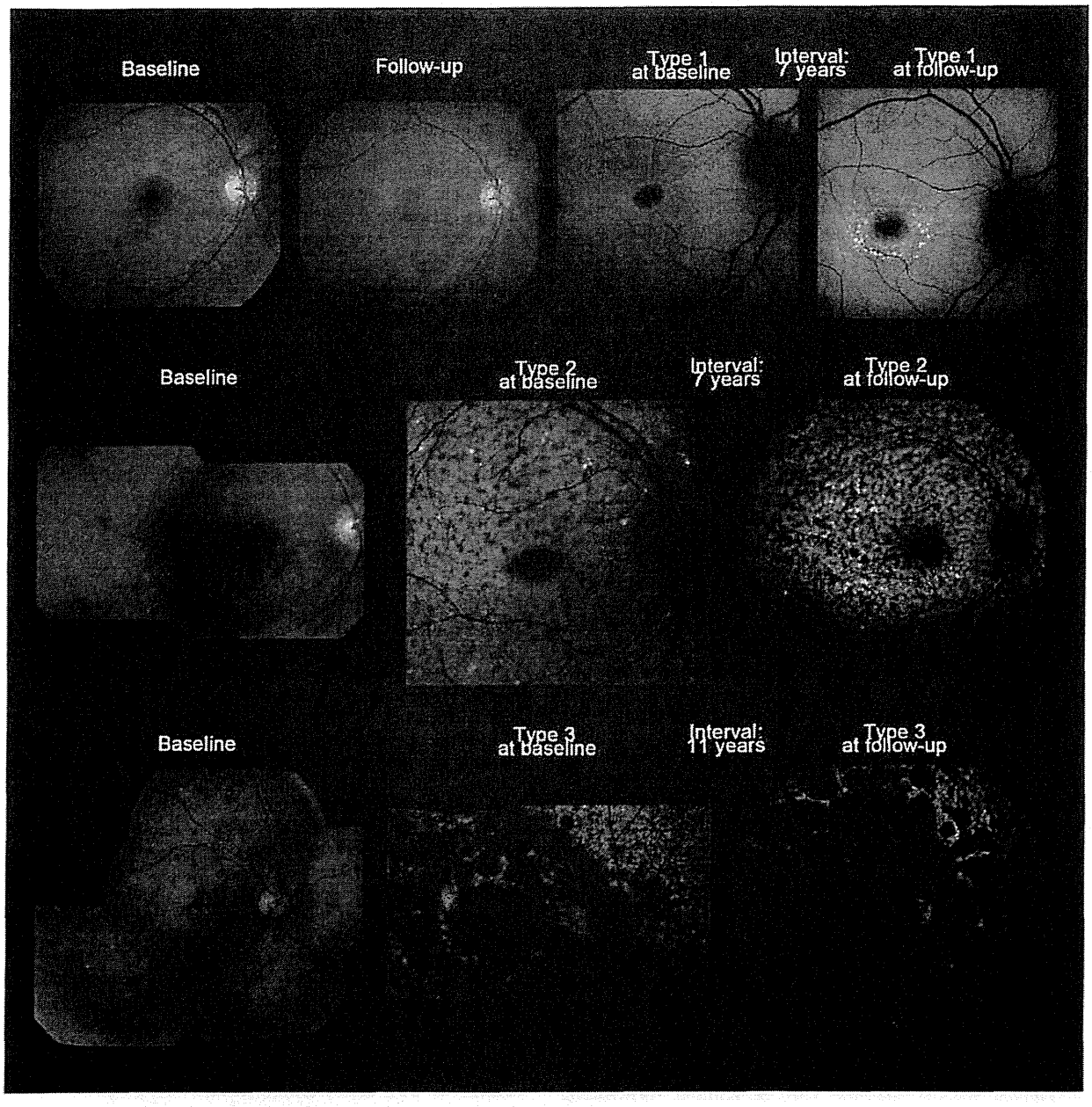

FIGURE 1. Color fundus photographs and AF images of three representative cases with Stargardt disease, illustrating the three AF subtypes in subjects where there was no subtype transition over time (patients 7, 50, and 54). *Top row*: Color fundus photographs of patient 7 showing subtle RPE changes at the fovea at baseline with a mild increase in the degree of atrophy at follow-up. AF imaging demonstrates a localized low signal lesion with a relatively high signal edge and a homogeneous background at baseline, and a low signal foveal lesion surrounded by patchy small foci with high signal and a homogeneous background at follow-up; consistent with AF type 1 at baseline and follow-up. *Middle row*: Patient 50 had macular atrophy surrounded by yellowish-white flecks extending anterior to the vascular arcades at baseline, and a low signal area at the macula surrounded by high and low foci throughout the posterior pole (AF type 2) at baseline and follow-up, with a heterogeneous background at baseline and follow-up. *Bottom row*: Patient 65 had extensive areas of atrophy throughout the posterior pole, extending beyond the vascular arcades, with yellowish-white and atrophic flecks at baseline, and multiple areas of low signal with heterogeneous background (AF type 3) at baseline and follow-up.

Where possible, AF images with a 30° × 30° field were used for RAE analysis ($n = 68$ at baseline and $n = 67$ at follow-up). For patients with AF images available in both eyes at baseline and follow-up ($n = 61$), the eye used for analysis was selected according to the Random Integer Generator (available in the public domain at http://www.random.org/), and for individuals with AF imaging available in only one eye ($n = 7$), that eye was selected for analysis. Patients who had central atrophy that extended beyond the limits of the AF images obtained with field of view 30° × 30° were excluded from the size of atrophy and RAE analyses ($n = 6$).

TABLE 1. Definition of Fundus AF Subtypes in Stargardt Disease

Type 1	Localized low AF signal at the fovea surrounded by a homogeneous background with/without perifoveal foci of high or low signal
Type 2	Localized low AF signal at the macula surrounded by a heterogeneous background and widespread foci of high or low AF signal extending anterior to the vascular arcades
Type 3	Multiple areas of low AF signal at posterior pole with a heterogeneous background with/without foci of high or low signal

It has been challenging in Stargardt disease to establish comprehensive genotype–phenotype correlations due to the variable phenotype and the heterogeneity of *ABCA4*; more than 700 sequence variants have been reported.[1,2,9-15,31-44] A previous cross-sectional study of 43 patients with Stargardt disease demonstrated that AF patterns appeared to relate to functional abnormalities.[5] A recent small AF study ($n = 12$) demonstrated variable rates of enlargement of RPE atrophy in Stargardt disease, with a strong association between atrophy enlargement and electrophysiological grouping.[6] Chen et al.[30] also have reported the progressive change in the area of atrophy in 52 patients with Stargardt disease over a mean follow-up of 2.92 years; with variable atrophy progression demonstrated, and an association with electrophysiological findings. However, comprehensive investigations over a long-term follow-up of a large cohort of patients with Stargardt disease, including AF imaging, clinical assessment, and molecular analysis still are lacking.

The purpose of this study was to characterize the subtypes of AF and investigate the enlargement of RPE atrophy in patients with Stargardt disease in a longitudinal survey with a mean follow-up of 9 years. This study also provided an opportunity to investigate the association of these AF subtypes and atrophy progression with the detailed clinical and molecular genetic findings.

METHODS

Patients

A cohort of 68 patients with a clinical diagnosis of Stargardt disease and a minimum of 6 years of follow-up were ascertained at Moorfields Eye Hospital.

For the purpose of this study, patients with a clinical history compatible with Stargardt disease and clinical signs of bilateral macular atrophy, with or without surrounding flecks, were included. The clinical features of 42 patients in this cohort have been described partially in an earlier report, which did not include AF findings.[9] The panel included five sibling pairs. After informed consent was obtained, blood samples were taken for DNA extraction and mutation screening of *ABCA4*. The protocol of the study adhered to the provisions of the Declaration of Helsinki and was approved by the local Ethics Committee of Moorfields Eye Hospital.

Clinical Assessment

We assessed 68 patients on at least two occasions, with the first and most recent visits taken as the baseline and "follow-up" examinations, respectively, for the purposes of data analysis. A full medical history was obtained and a comprehensive ophthalmologic examination performed. The age of onset was defined as the age at which visual loss was first noted by the patient. The duration of the disease was calculated as the difference between age at onset and age at the baseline examination when AF imaging was obtained. The interval of observation was determined by the difference between the age at baseline and the age at the most recent "follow-up" examination when AF imaging was done.

Best-corrected Snellen visual acuity was converted to equivalent logMAR visual acuity,[45] and visual acuity reduction was calculated as the difference between logMAR visual acuity at baseline and follow-up.

Fundus AF Imaging

The AF imaging was performed using a confocal scanning laser ophthalmoscope (cSLO). Baseline images were obtained before 2003 using a Zeiss prototype cSLO (SM 30-4024, excitation light 488 nm, barrier filter 521 nm, field of view 30° × 30°; Carl Zeiss Meditec, Oberkochen, Germany).[5,29,46-48] From 2003 to 2009, images were obtained using an HRA2 (excitation light 488 nm, barrier filter 500 nm, field of view 30° × 30°; Heidelberg Engineering GmbH, Heidelberg, Germany).[47] After 2009, images were obtained using the Spectralis with viewing module version 5.1.2.0 (excitation light 488 nm, barrier filter 500 nm, fields of view 30° × 30° and 55° × 55°; Heidelberg Engineering GmbH).[49]

Patients were classified into 3 AF subtypes based on a recent report of AF findings in Stargardt disease:[10] type 1 – localized low AF signal at the fovea surrounded by a homogeneous background, with/without perifoveal foci of high or low AF signal; type 2 – localized low AF signal at the macula surrounded by a heterogeneous background, and widespread foci of high or low AF signal extending anterior to the vascular arcades; and type 3 – multiple areas of low AF signal at the posterior pole with a heterogeneous background, with/without foci of high or low AF signal (Table 1, Fig. 1). In previously published reports, the progression of atrophy has been influenced by two patterns of background AF ("homogeneous" and "heterogeneous"),[6] and multiple atrophic lesions at the posterior pole have been associated with a more rapid functional deterioration.[9] The data of AF subtypes obtained at follow-up were compared to those at baseline. A patient (patient 61) who had an asymmetric AF subtype was excluded from the AF subtype analysis.

Areas of low AF signal were measured using custom software (Retinal analysis tool; Halfyard AS, Fitzke FW, University College London [UCL] Institute of Ophthalmology, London, UK). With reference to a given distance between the center of the optic nerve head and the foveola, which is defined as 15°, this software enables measurement of the dimensions of the area tracked manually and computation of the size expressed in square degrees automatically (Fig. 2). The significant low gray scale point on the images was decided upon by agreement between the two investigators (KF, RM) and the dimension of the area within the tracked line of low gray scale was calculated.

All the values in square degrees were converted to square millimeters using the previously reported conversion factor (1° = 0.3 mm; Fitzke FW. *IOVS* 1981;20(suppl):ARVO Abstract 144). Only low AF signal lesions of >0.18 mm^2 in size were considered. The total area of atrophy was calculated by summation of all the measured low signal lesions. All of these measurements were conducted by two investigators (KF, RM), and the averaged values were used for final analyses. The rate of atrophy enlargement (RAE, mm^2/y) was calculated as follows according to previous reports[6,30]: size of the area of atrophy at last follow-up minus size of the area of atrophy at baseline (mm^2) divided by the follow-up time (years) (Fig. 2).

A Longitudinal Study of Stargardt Disease: Quantitative Assessment of Fundus Autofluorescence, Progression, and Genotype Correlations

Kaoru Fujinami,[1-4] Noemi Lois,[5] Rajarshi Mukherjee,[1,2] Vikki A. McBain,[6] Kazushige Tsunoda,[3] Kazuo Tsubota,[4] Edwin M. Stone,[7] Fred W. Fitzke,[1] Catey Bunce,[1,2] Anthony T. Moore,[1,2] Andrew R. Webster,[1,2] and Michel Michaelides[1,2]

[1]University College London Institute of Ophthalmology, London, United Kingdom
[2]Moorfields Eye Hospital, London, United Kingdom
[3]Laboratory of Visual Physiology, National Institute of Sensory Organs, National Hospital Organization, National Tokyo Medical Center, Meguro-ku, Tokyo, Japan
[4]Department of Ophthalmology, Keio University School of Medicine, Shinjyuku-ku, Tokyo, Japan
[5]Clinical Ophthalmology at the Centre for Vision and Vascular Science, Queens University Belfast, Belfast, Northern Ireland
[6]Department of Ophthalmology, Institute of Medical Sciences, University of Aberdeen, Aberdeen, Scotland, United Kingdom
[7]University of Iowa, Institute for Vision Research, Howard Hughes Medical Institute, Iowa City, Iowa

Correspondence: Michel Michaelides, UCL Institute of Ophthalmology, 11-43 Bath Street, London EC1V 9EL, UK;
michel.michaelides@ucl.ac.uk.

Submitted: March 26, 2013
Accepted: November 8, 2013

Citation: Fujinami K, Lois N, Mukherjee R, et al. A longitudinal study of Stargardt disease: quantitative assessment of fundus autofluorescence, progression, and genotype correlations. *Invest Ophthalmol Vis Sci.* 2013;54:8181–8190. DOI:10.1167/iovs.13-12104

Purpose. We characterized subtypes of fundus autofluorescence (AF) and the progression of retinal atrophy, and correlated these findings with genotype in Stargardt disease.

Methods. Full clinical examination and AF imaging was undertaken in 68 patients with Stargardt disease. The baseline data were compared to those at follow-up. Patients were classified into three AF subtypes: type 1 had a localized low signal at the fovea surrounded by a homogeneous background, type 2 had a localized low signal at the macula surrounded by a heterogeneous background with numerous foci of abnormal signal, and type 3 had multiple low signal areas at the posterior pole with a heterogeneous background. At baseline, there were 19 patients with type 1, 41 with type 2, and 8 with type 3 disease. The areas of reduced AF signal were measured and rate of atrophy enlargement (RAE) was calculated as the difference of the atrophy size over time (mm^2) divided by the follow-up interval (years). Molecular screening of *ABCA4* was undertaken.

Results. The mean follow-up interval was 9.1 years. A total of 42% cases with type 1 disease progressed to type 2, and 12% with type 2 progressed to type 3. The RAE (mm^2/y) based upon baseline AF subtypes was significantly different; 0.06 in type 1, 0.67 in type 2, and 4.37 in type 3. *ABCA4* variants were identified in 57 patients. There was a significant association between AF subtype and genotype.

Conclusions. The AF pattern at baseline influences the enlargement of atrophy over time and has genetic correlates. These data are likely to assist in the provision of counseling on prognosis in Stargardt disease and be valuable for future clinical trials.

Keywords: Stargardt, ABCA4, autofluorescence

Stargardt disease is the most common inherited macular dystrophy, and is associated with a variable phenotype and disease severity.[1-12] Stargardt disease typically presents with central macular atrophy and yellow-white flecks at the posterior pole, primarily at the level of the RPE. Progressive retinal degeneration over time, including development/resorption of flecks, atrophy enlargement, and deterioration of retinal function, has been reported in Stargardt disease.[7-9] Mutations in the gene *ABCA4* underlie Stargardt disease, and also have been implicated in cone dystrophy, cone-rod dystrophy, and "retinitis pigmentosa."[2,9,10,13-17] The *ABCA4* gene encodes a transmembrane rim protein in the outer segment discs of photoreceptors that is involved in active transport of retinoids from photoreceptor to RPE.[18-24] Failure of this transport results in accelerated deposition of a major lipofuscin fluorophore, N-retinylidene-N-retinylethanolamine (A2E), in the RPE.[20-22] A2E and other lipofuscin fluorophores are elevated dramatically in the RPE of postmortem samples from patients with Stargardt disease and in *ABCA4* knockout mice (*abca4*$^{-/-}$).[19,25] Over time, A2E-associated cytotoxicity is believed to cause RPE dysfunction and cell death, with subsequent photoreceptor cell loss.[26,27]

Autofluorescence (AF) imaging can provide useful information about the distribution of lipofuscin in the RPE, and give indirect information on the level of metabolic activity of the RPE; lipofuscin levels are determined largely by the rate of turnover of photoreceptor outer segments.[28,29] The abnormal accumulation of lipofuscin, the presence of active and resorbed flecks, and RPE atrophy leads to a characteristic appearance on AF imaging in Stargardt disease; very low AF signals in photoreceptor and RPE atrophy, and foci with low or high AF signals due to flecks.[5,6,10,30]

SUPPLEMENTAL TABLE 7. *Investigation of the Pathogenicity of Identified ABCA4 Variants (Continued)*

				SIFT[a]		PolyPhen 2[a]		HSF Matrix[a]					
Exon	Nucleotide Substitution and Amino Acid Change	Number of Alleles	Previous Report	Pred.	Index (0-1)	Pred.	Hum Var Score (0-1)	Site Affected	Wt CV	Mt CV	CV % Variation	Allelic Frequency Observed by EVS[a]	Reference
43	c.5908 C>T, p.Leu1970Phe	1	Lewis[25]	Tol.	0.14	PRD	0.997				No change	ND	
44	c.6079 C>T, p.Leu2027Phe	4	Allikmets[11]	Intol.	0.02	PRD	0.999				No change	3/10 758	db SNP (rs61751408)
44	c.6089 G>A, p.Arg2030Gln	2	Lewis[25]	Tol.	0.1	PRD	0.999				No change	6/10 758	db SNP (rs61750641)
46	c.6320 G>A, p.Arg2107His	2	Fishman[21]	Intol.	0	PRD	0.996				NA	83/10 758	db SNP (rs62642564)
47	c.6449 G>A, p.Cys2150Tyr	5	Fishman[21]	Intol.	0	PRD	0.995	Don.	76.6	49.8	Site broken (−35.02)	1/10 758	db SNP (rs61751384)

Acc. = acceptor site; Don. = donor site; EVS = Exome Variant Server; HSF = Human Splicing Finder program; Hum Var = Human Var score; Int. = intron; Intol. = intolerant; Mt CV = mutant consensus value; NA = not applicable; ND = not detected; PRD = probably damaging; Pred. = prediction; SIFT = Sorting Intolerant from Tolerance program; Tol. = tolerant; Wt CV = wild-type consensus value.

[a]SIFT (version 4.0.4) results are reported to be tolerant if tolerance index ≥ 0.05 or intolerant if tolerance index < 0.05. PolyPhen-2 (version 2.1) appraises mutations qualitatively as Benign, Possibly Damaging, or Probably Damaging based on the model's false-positive rate. The cDNA is numbered according to Ensembl transcript ID ENST00000370225, in which +1 is the A of the translation start codon. Human Splicing Finder (HSF, version 2.4.1) reports the results from the HSF matrix: the higher the consensus value (CV), the stronger the predicted splice site. The values for the wild-type and mutant sequences are shown; the larger the difference between these values, the greater the chance that the variant can affect splicing. EVS denotes variants in the Exome Variant Server, NHLBI Exome Sequencing Project, Seattle, WA, USA (accessed January 12, 2012; http://snp.gs.washington.edu/EVS/).

SUPPLEMENTAL TABLE 7. Investigation of the Pathogenicity of Identified *ABCA4* Variants

Exon	Nucleotide Substitution and Amino Acid Change	Number of Alleles	Previous Report	SIFT* Pred.	SIFT* Index (0-1)	PolyPhen 2* Pred.	PolyPhen 2* Hum Var Score (0-1)	HSF Matrix† Site Affected	HSF Matrix† Wt CV	HSF Matrix† Mt CV	HSF Matrix† CV % Variation	Allelic Frequency Observed by EVS‡	Reference
3	c.161 G>A, p.Cys54Tyr	3	Lewis[25]	Tol.	0.11	PRD	0.994				No change	1/10 758	db SNP (rs150774447)
3	c.286 A>C, p.Asn96His	1	Papaioannou[26]	Tol.	0.14	PRD	0.994				No change	1/10 758	db SNP (rs61748529)
5	c. 466 A>G, p. Ile156 Val	2	Papaioannou[26]	Tol.	0.46	Benign	0.003				No change	11/10 758	db SNP (rs112467008)
6	c.758 G>T, p.Val256Val/Splice site	1	Klevering[24]	Tol.	0.56	NA		Don.	70.4	58	Site broken (−17.51)	ND	
9	c.1222 C>T, p.Arg408*	1	Webster[29]	NA		NA							
10	c.1253 T>C, p.Phe418Ser	1	Zernant[30]	Intol.	0	PRD	0.99				No change	ND	
10	c.1317 G>A, p.Trp439*	2	This study	NA		NA						ND	
12	c.1721delAC, p.Asp574Aspfs*582	1	Briggs[20]	NA		NA		Acc.	47.2	68.3	New site (44.5)	ND	
14	c.1957 C>T, p.Arg653Cys	1	Rivera[27]	Tol.	0.1	PRD	0.999				No change	1/10 758	db SNP (rs141823837)
14	c.2023 G>A, p.Val675Ile	1	This study	Tol.	0.07	PRD	0.989				NA	ND	
15	c.2239delC, p.Leu747Cysfs*787	1	This study	NA		NA		Don.	34.7	77	New site (−122)	ND	
17	c.2588 G>C, p.Gly863Ala	8	Allikmets[11]	Intol.	0.01	PRD	0.996				No change	53/10 758	db SNP (rs76157638)
19	c.2791 G>A, p.Val931Met	1	Allikmets[10]	Tol.	0.12	PRD	0.716				No change	18/10 758	db SNP (rs58331765)
19	c.2828 G>A, p.Arg943Gln	3	Webster[29]	Intol.	0.03	Benign	0.449	Acc.	52.2	81.1	New site (+55.48)	340/10 758	db SNP (rs1801581)
19	c.2894 A>G, p.Asn965Ser	1	Lewis[25]	Intol.	0	PRD	0.981	Acc.	53.4	82.3	New site (+54.26)	ND	
21	c.3056 C>T, p.Thr1019Met	2	Rozet[28]	Intol.	0	PRD	0.999				No change	ND	
22	c.3211_3212insGT, p.Ser1071Cysfs*1084	2	Allikmets[10]	NA		NA		Don.	69.3	28	Site broken (−59.55)	ND	
22	c.3259 G>A, p.Glu1087Lys	1	Lewis[25]	Intol.	0	PRD	0.997				No change	ND	
22	c.3322 C>T, p.Arg1108Cys	2	Rozet[28]	Intol.	0	PRD	0.986				No change	1/10 758	db SNP (rs61750120)
22	c.3323 G>A, p.Arg1108His	1	Webster[29]	Intol.	0	PRD	0.986				No change	ND	
28	c.4139 C>T, p.Pro1380Leu	4	Lewis[25]	Intol.	0.01	Benign	0.377				No change	2/10 758	db SNP (rs61750130)
Int. 28	c.4253+5 G>T, Splice site	1	Lewis[25]	NA		NA		Don.	87.9	75.6	Site broken (−14.02)	1/10 758	
29	c.4328 G>A, p.Arg1443His	1	Jaakson[23]	Tol.	0.19	PRD	0.996				No change	ND	
30	c. 4363 C>T, p. Cys1455Arg	1	This study	Tol.	0.34	PRD	0.994				NA	ND	
30	c.4469 G>A, p.Cys1490Tyr	1	Webster[29]	Intol.	0.03	PRD	0.994				No change	ND	
30	c.4519 G>A, p.Gly1507Arg	1	This study	Tol.	0.48	PRD	0.996	Acc.	78.9	78.9	New site (+58.11)	ND	
30	c.4537_4538insC, p.Gly1513Profs*1554	1	Briggs[20]	NA		NA		Acc.	91.7	33.3	Site broken (−63.76)	ND	
35	c.4918 C>T, p.Arg1640Trp	1	Rozet[28]	Intol.	0	PRD	1				No change	ND	
35	c.4956 T>G, p.Tyr1652*	1	Fumagalli[22]	NA		NA							
Int. 35	c.5461-10 T>C	9	Briggs[20]	NA		NA						3/10 758	db SNP (rs1800728)
39	c. 5516 T>C, p. Phe1839Ser	1	This study	Intol.	0	PRD	0.988				No change	ND	
Int. 40	c.5714+5 G>A, Splice site	1	Cremers[13]	NA		NA		Donor	85.5	73.3	Wild-type site broken (−14.23)	ND	
42	c.5882 G>A, p.Gly1961Glu	1	Allikmets[11]	Tol.	0.18	PRD	1				No change	29/10 758	db SNP (rs1800553)

Continued on next page

SUPPLEMENTAL TABLE 6. Electrophysiologic Group Transition and ABCA4 Variantsa Identified in 59 Patients With Stargardt Disease (*Continued*)

Pt	Electrophysiologic Group (BL / FU)	Genotype Group	Number of Variants	Exon	Nucleotide Substitution	Amino Acid Change	Screening Method (Yes/No)		
							SSCP	APEX	DS
35	II / II	B	2	3	c.161 G>A	p.Cys54Tyr	✓	—	—
				17	c.2588 G>C	p.Gly863Ala	✓	—	—
36	II / II	A	2	19	c.2791 G>A	p.Val931Met	—	✓	—
				Int. 38	c.5461-10 T>C	Splice site	—	✓	—
37	II / III	C	1	28	c.4139 C>T	p.Pro1380Leu	—	✓	—
38	II / III	A	2	22	c.3211_3212insGT	p.Ser1071Cysfs*1084	—	✓	—
				28	c.4139 C>T	p. Pro1380Leu	—	✓	—
39	II / III	A	2	Int. 38	c.5461-10 T>C	Splice site	—	✓	—
				Int. 40	c.5714+5 G>A	Splice site	—	✓	—
40	II / III	D	0				✓	—	—
41	II / III	D	0				✓	—	—
42	II / III	C	1	3	c.161 G>A	p.Cys54Tyr	✓	—	—
43	II / III	D	0				✓	—	—
44	II / III	C	1	19	c.2894 A>G	p.Asn965Ser	✓	—	—
45	III / III	C	1	21	c.3056 C>T	p.Thr1019Met	✓	—	—
46	III / III	C	1	21	c.3056 C>T	p.Thr1019Met	✓	—	—
47	III / III	C	1	47	c.6449 G>A	p.Cys2150Tyr	✓	—	✓
48	III / III	A	2	Int. 38	c.5461-10 T>C	Splice site	—	✓	—
				44	c.6079 C>T	p.Leu2027Phe	—	✓	—
49	III / III	A	1	12	c.1721delAC	p.Asp574Aspfs*582	✓	—	—
50	III / III	A	1	Int. 38	c.5461-10 T>C	Splice site	—	✓	—
51	III / III	B	2	35	c.4918 C>T	p.Arg1640Trp	✓	—	—
				44	c.6079 C>T	p.Leu2027Phe	✓	—	—
52	III / III	C	1	22	c.3323 G>A	p.Arg1108His	✓	—	—
53	III / III	A	2	Int. 38	c.5461-10 T>C	Splice site	—	—	✓
				47	c.6449 G>A	p.Cys2150Tyr	✓	—	✓
54	III / III	A	2	Int. 38	c.5461-10 T>C	Splice site	—	—	✓
				47	c.6449 G>A	p.Cys2150Tyr	✓	—	✓
55	III / III	A	2	Int. 38	c.5461-10 T>C	Splice site	—	✓	✓
				47	c.6449 G>A	p.Cys2150Tyr	—	✓	✓
56	III / III	D	0				✓	—	—
57	III / III	A	1	**15**	**c.2239delC**	**p.Leu747Cysfs*787**	✓	—	✓
58	III / III	D	0				✓	—	—
59	III / III	C	1	5	c.466 A>G	p.Ile156 Val	✓	—	—

✓ = yes; — = no; APEX = arrayed primer extension microarray; BL = baseline; DS = Sanger direct sequencing; FU = follow-up; Int. = intron; SSCP = single-strand conformation polymorphism.

[a]Putative novel changes are in bold. All the variants are heterogeneous.

SUPPLEMENTAL TABLE 6. Electrophysiologic Group Transition and *ABCA4* Variants[a] Identified in 59 Patients With Stargardt Disease

Pt	Electrophysiologic Group (BL / FU)	Genotype Group	Number of Variants	Exon	Nucleotide Substitution	Amino Acid Change	Screening Method (Yes/No)		
							SSCP	APEX	DS
1	I / I	A	3	6	c.768 G>T	p.Val256Val/ Splice site	✓	✓	—
				17	c.2588 G>C	p.Gly863Ala	✓	✓	—
				19	c.2828 G>A	p.Arg943Gln	—	✓	—
2	I / I	C	1	29	c.4328 G>A	p.Arg1443His	—	✓	—
3	I / I	A	3	**10**	**c.1317 G > A**	**p.Trp439***	—	✓	✓
				17	c.2588 G>C	p.Gly863Ala	—	✓	✓
				43	c.5908 C>T	p.Leu1970Phe	—	✓	✓
4	I / I	C	1	44	c.6079 C>T	p.Leu2027Phe	—	✓	—
5	I / I	A	3	17	c.2588 G>C	p.Gly863Ala	—	✓	—
				19	c.2828 G>A	p.Arg943Gln	—	✓	—
				Int. 38	c.5461-10 T>C	Splice site	—	✓	—
6	I / I	C	1	28	c.4139 C>T	p.Pro1380Leu	—	✓	—
7	I / I	D	0				✓	—	—
8	I / I	B	2	10	c.1253 T>C	p.Phe418Ser	✓	—	✓
				44	c.6079 C>T	p.Leu2027Phe	✓	—	✓
9	I / I	A	2	Int. 28	c.4253+5 G>T	Splice site	✓	✓	—
				30	**c.4519 G > A**	**p.Gly1507Arg**	✓	—	✓
10	I / I	B	2	30	c.4469 G>A	p.Cys1490Tyr	—	✓	✓
				44	c.6089 G>A	p.Arg2030Gln	—	✓	✓
11	I / I	D	0				—	✓	—
12	I / I	C	1	3	c.286 A>C	p.Asn96His	✓	—	—
13	I / I	A	1	30	c.4537_4538insC	p.Gly1513Profs*1554	—	✓	—
14	I / I	D	0				✓	—	—
15	I / I	C	1	46	c.6320 G>A	p.Arg2107His	✓	—	—
16	I / I	D	0				—	✓	—
17	I / I	C	1	3	c.161 G>A	p.Cys54Tyr	✓	—	—
18	I / I	B	2	28	c.4139 C>T	p.Pro1380Leu	—	✓	—
				42	c.5882 G>A	p.Gly1961Glu	—	✓	—
19	I / I	C	1	22	c.3322 C>T	p.Arg1108Cys	✓	—	—
20	I / I	A	2	**10**	**c.1317 G > A**	**p.Trp439***	—	✓	✓
				17	c.2588 G>C	p.Gly863Ala	—	✓	✓
21	I / I	B	3	5	c. 466 A>G	p. Ile156 Val	✓	—	✓
				30	**c. 4363 C > T**	**p. Cys1455Arg**	✓	—	✓
				39	**c. 5516 T > C**	**p. Phe1839Ser**	✓	—	✓
22	I / II	C	1	46	c.6320 G>A	p.Arg2107His	—	✓	—
23	I / II	C	1	17	c.2588 G>C	p.Gly863Ala	—	✓	—
24	I / II	A	1	35	c.4956 T>G	p.Tyr1652*	—	✓	—
25	I / III	A	1	Int. 38	c.5461-10 T>C	Splice site	—	✓	—
26	I / III	D	0				✓	—	—
27	I / III	A	1	22	c.3211_3212insGT	p.Ser1071Cysfs*1084	—	✓	—
28	II / II	A	2	9	c.1222 C>T	p.Arg408*	✓	—	✓
				14	**c.2023 G > A**	**p.Val675Ile**	✓	—	✓
29	II / II	C	1	47	c.6449 G>A	p.Cys2150Tyr	—	—	✓
30	II / II	D	0				—	✓	—
31	II / II	B	3	17	c.2588G>C	p.Gly863Ala	✓	—	—
				22	c.3322 C>T	p.Arg1108Cys	✓	—	—
				19	c.2828 G>A	p.Arg943Gln	✓	—	—
32	II / II	B	2	14	c.1957 C>T	p.Arg653Cys	—	✓	—
				44	c.6089 G>A	p.Arg2030Gln	—	✓	—
33	II / II	D	0				✓	—	—
34	II / II	B	2	17	c.2588 G>C	p.Gly863Ala	✓	—	—
				22	c.3259 G>A	p.Glu1087Lys	✓	—	—

Continued on next page

SUPPLEMENTAL TABLE 5. Detailed Results of Statistical Analysis[a] of Onset of Disease, Duration of Disease, Age at Baseline and Follow-up, Interval of Follow-up, logMAR Visual Acuity, logMAR Visual Acuity Reduction, Yearly Amplitude Reduction, and Yearly Peak Time Shift, With Respect to Electrophysiologic Group at Baseline, Electrophysiologic Deterioration, and Genotype Group

	Electrophysiologic Group at Baseline						Electrophysiologic Deterioration	Genotype Group						
	KW			KW S-D *P* Value			MW *P* Value	MW *P* Value	KW			KW S-D *P* Value			MW *P* Value
Onset of Disease															
χ^2	DOF	*P* Value	Gp1	Gp2	0.326	.155	.034*	χ^2	DOF	*P* Value	GtA	GtB	.091	.038*
14.3	2	.001**	Gp1	Gp3	0.001	.000**		14.3	2	.001**	GtA	GtC	.897	.660
			Gp2	Gp3	0.047	.018*					GtA	GtC	.101	.042*
Duration of Disease														
χ^2	DOF	*P* Value	Gp1	Gp2	.9648		.879	χ^2	DOF	*P* Value	GtA	GtB	.835	
2.2	2	.337	Gp1	Gp3	.3764			3.3	2	.191	GtA	GtC	.247	
			Gp2	Gp3	.4104						GtA	GtC	.312	
Age at Baseline														
χ^2	DOF	*P* Value	Gp1	Gp2	.6044		.283	χ^2	DOF	*P* Value	GtA	GtB	.390	
1.3	2	.521	Gp1	Gp3	.6173			3.3	2	.193	GtA	GtC	.677	
			Gp2	Gp3	.9982						GtA	GtC	.201	
Interval of Follow-up														
χ^2	DOF	*P* Value	Gp1	Gp2	.2904		.272	χ^2	DOF	*P* Value	Gt A	GtB	.921	
5.7	2	.057	Gp1	Gp3	.3833			0.8	2	.668	Gt A	GtC	.627	
			Gp2	Gp3	.0579						Gt A	GtC	.960	
logMAR VA at Baseline														
χ^2	DOF	*P* Value	Gp1	Gp2	.3623	.175	.002**	χ^2	DOF	*P* Value	GtA	GtB	.276	
12.0	2	.003**	Gp1	Gp3	.0029	.001**		3.4	2	.181	GtA	GtC	.261	
			Gp2	Gp3	.0536	.021*					GtA	GtC	.975	
logMAR VA Reduction														
χ^2	DOF	*P* Value	Gp1	Gp2	.7266		.510	χ^2	DOF	*P* Value	GtA	GtB	.938	
1.3	2	.513	Gp1	Gp3	.8456			1.0	2	.605	GtA	GtC	.768	
			Gp2	Gp3	.4994						GtA	GtC	.582	
Yearly Amplitude Reduction for Dark-Adapted 11.0 A-wave														
χ^2	DOF	*P* Value	Gp1	Gp2	.9769	.6153	.013*	χ^2	DOF	*P* Value	GtA	GtB	.042	.0162*
6.3	2	.042*	Gp1	Gp3	.0631	.0248*		7.7	2	.022*	GtA	GtC	.181	.0794
			Gp2	Gp3	.0687	.0272*					GtA	GtC	.201	.0896
Yearly Peak Time Shift for Dark-Adapted 11.0 A-wave														
χ^2	DOF	*P* Value	Gp1	Gp2	.9619		.008**	χ^2	DOF	*P* Value	GtA	GtB	.303	
2.1	2	.343	Gp1	Gp3	.4272			2.4	2	.308	GtA	GtC	.973	
			Gp2	Gp3	.3632						GtA	GtC	.382	
Yearly Amplitude Reduction for Light-Adapted 30 Hz														
χ^2	DOF	*P* Value	Gp1	Gp2	.5895		.407	χ^2	DOF	*P* Value	GtA	GtB	.201	
1.6	2	.450	Gp1	Gp3	.9065			3.6	2	.166	GtA	GtC	.996	
			Gp2	Gp3	.4674						GtA	GtC	.183	
Yearly Peak Time Shift for Light-Adapted 30 Hz														
χ^2	DOF	*P* Value	Gp1	Gp2	.5452	.2969	.000**	χ^2	DOF	*P* Value	GtA	GtB	.617	
5.3	2	.072	Gp1	Gp3	.0708	.0283*		4.7	2	.094	GtA	GtC	.339	
			Gp2	Gp3	.3395	.1634					GtA	GtC	.091	

DOF = degree of freedom; Gp = group; Gt = genotype; KW = Kruskal-Wallis; MW = Mann-Whitney test; S-D = Steel-Dwass.

The Mann-Whitney *U* test was also applied to study the parameters in terms of which the Kruskal-Wallis test detected significant differences between electrophysiologic groups or genotype groups. *for $P < .05$ and **for $P < .01$ are used to identify statistically significant differences.

[a]The Kruskal-Wallis test with Steel-Dwass multiple comparisons was performed to compare the 3 electrophysiologic groups and 3 genotype groups in all combinations. The Mann-Whitney *U* test was applied to investigate the differences between subsets with/without evidence of clinically significant electrophysiologic deterioration.

SUPPLEMENTAL TABLE 4. Detailed Electrophysiologic Findings of 59 Patients With Stargardt Disease: Electrophysiologic Group, Electrophysiologic Deterioration, and Assessment of Each Component of Full-field Electroretinography (*Continued*)

Pt	Selected Eye for Data Analysis	Electrophysiologic Group		Electrophysiologic Deterioration			Dark-Adapted 0.01 (R/L)		Dark-Adapted 11.0 (R/L)		Light-Adapted 30 Hz (R/L)		Light-Adapted 3.0 (R/L)	
		BL	FU	Yes/No	Amplitude Reduction	Peak Time Shift	BL	FU	BL	FU	BL	FU	BL	FU
37	L	2	3	✓	✓	✓	N/N	N/N	N/N	A/A	A/A	A/A	A/A	A/A
38	L	2	3	✓	✓	✓	N/N	A/A	N/N	A/A	A/A	A/A	A/A	A/A
39	R	2	3	✓	—	✓	N/N	NA/NA	N/N	A/A	A/A	A/A	A/A	A/A
40	L	2	3	✓	✓	✓	N/N	A/A	N/N	A/A	N/N	A/A	A/A	A/A
41	R	2	3	✓	—	✓	N/N	A/A	N/N	A/A	N/N	A/A	N/A	A/A
42	L	2	3	✓	✓	—	N/N	A/A	N/N	A/A	A/A	A/A	N/N	A/A
43	L	2	3	✓	✓	—	N/N	A/A	N/N	A/A	A/A	A/A	A/A	A/A
44	R	2	3	✓	✓	✓	N/N	A/A	N/N	A/A	A/A	A/A	A/A	A/A
45	R	3	3	✓	✓	✓	NA/NA	A/A	A/A	A/A	A/A	A/A	A/A	A/A
46	L	3	3	✓	—	✓	NA/NA	N/N	A/A	A/A	A/A	A/A	A/A	A/A
47	R	3	3	✓	—	✓	NA/NA	A/A	A/A	A/A	A/A	A/A	A/A	A/A
48	R	3	3	✓	✓	—	N/N	A/A	N/A	A/A	A/A	A/A	N/N	A/A
49	L	3	3	✓	✓	✓	A/A	A/A	A/A	A/A	A/A	A/A	A/A	A/A
50	R	3	3	✓	✓	✓	A/A	A/A	A/A	A/A	A/A	A/A	A/A	A/A
51	R	3	3	✓	—	✓	A/A	A/A	A/A	A/A	A/A	A/A	A/A	A/A
52	L	3	3	✓	✓	✓	A/A	A/A	A/A	A/A	A/A	A/A	A/A	A/ND
53	L	3	3	✓	✓	✓	A/A	ND/ND	A/A	A/A	ND/ND	ND/ND	ND/ND	ND/ND
54	R	3	3	✓	✓	✓	A/A	ND/ND	A/A	A/A	ND/ND	ND/ND	ND/ND	ND/ND
55	L	3	3	✓	✓	—	A/A	ND/ND	A/A	A/A	A/A	ND/ND	A/A	ND/ND
56	R	3	3	✓	✓	—	A/A	ND/ND	A/A	ND/ND	ND/ND	ND/ND	ND/ND	ND/ND
57	L	3	3	✓	✓	✓	A/A	A/A	A/A	A/A	A/A	A/A	A/A	A/A
58	L	3	3	✓	—	✓	A/A	A/A	A/A	A/A	A/A	A/A	A/A	A/A
59	L	3	3	✓	✓	✓	A/A	A/A	N/A	A/A	N/A	A/A	N/A	A/A

✓ = yes; — = no; A = Abnormal; BL = baseline; Dark-adapted 0.01 = dark-adapted dim flash electroretinogram with flash intensity 0.01 candela second (cd·s)/m^2; Dark-adapted 11.0 = dark-adapted bright flash electroretinogram with flash intensity 11.0 cd·s/m^2; FU = follow-up; L = left; Light-adapted 30 Hz = light-adapted 30 Hz flicker electroretinogram with flash intensity 3.0 cd·s/m^2; Light-adapted 3.0 = light-adapted 2 Hz electroretinogram with flash intensity 3.0 cd·s/m^2; N = normal; NA = not available; ND = not-detectable; Pt = patient; R = right; VA = visual acuity.

SUPPLEMENTAL TABLE 4. Detailed Electrophysiologic Findings of 59 Patients With Stargardt Disease: Electrophysiologic Group, Electrophysiologic Deterioration, and Assessment of Each Component of Full-field Electroretinography

Pt	Selected Eye for Data Analysis	Electrophysiologic Group		Electrophysiologic Deterioration			Dark-Adapted 0.01 (R/L)		Dark-Adapted 11.0 (R/L)		Light-Adapted 30 Hz (R/L)		Light-Adapted 3.0 (R/L)	
		BL	FU	Yes/No	Amplitude Reduction	Peak Time Shift	BL	FU	BL	FU	BL	FU	BL	FU
1	R	1	1	–	–	–	N/N	N/N	N/N	N/N	N/N	N/N	N/N	N/N
2	L	1	1	–	–	–	N/N	N/N	N/N	N/N	N/N	N/N	N/N	N/N
3	L	1	1	–	–	–	N/N	N/N	N/N	N/N	N/N	N/N	N/N	N/N
4	R	1	1	–	–	–	N/N	N/N	N/N	N/N	N/N	N/N	N/N	N/N
5	L	1	1	–	–	–	N/N	N/N	N/N	N/N	N/N	N/N	N/N	N/N
6	R	1	1	–	–	–	N/N	N/N	N/N	N/N	N/N	N/N	N/N	N/N
7	L	1	1	–	–	–	N/N	N/N	N/N	N/N	N/N	N/N	N/N	N/N
8	L	1	1	–	–	–	N/N	N/N	N/N	N/N	N/N	N/N	N/N	N/N
9	R	1	1	–	–	–	N/N	N/N	N/N	N/N	N/N	N/N	N/N	N/NA
10	R	1	1	–	–	–	N/N	N/N	N/N	N/N	N/N	N/N	N/N	N/N
11	R	1	1	–	–	–	N/N	N/N	N/N	N/N	N/N	N/N	N/N	N/N
12	L	1	1	–	–	–	N/N	N/N	N/N	N/N	N/N	N/N	N/N	N/N
13	L	1	1	–	–	–	N/N	N/N	N/N	N/N	NA/N	NA/N	N/N	N/N
14	L	1	1	–	–	–	N/N	N/N	N/N	N/N	N/N	N/N	N/N	N/N
15	R	1	1	–	–	–	N/N	N/N	N/N	N/N	N/N	N/N	N/N	N/N
16	R	1	1	–	–	–	N/N	N/N	N/N	N/N	N/N	N/N	N/N	N/N
17	L	1	1	–	–	–	N/N	N/N	N/N	N/N	N/N	N/N	N/N	N/N
18	L	1	1	–	–	–	N/N	N/N	N/N	N/N	N/N	N/N	NA/N	NA/N
19	L	1	1	–	–	–	N/N	N/N	N/N	N/N	N/N	N/N	N/N	N/N
20	R	1	1	–	–	–	N/N	N/N	N/N	N/N	N/N	N/N	N/N	N/N
21	L	1	1	–	–	–	NA/NA	N/N	N/N	N/N	N/N	N/N	N/N	N/N
22	R	1	2	✓	–	✓	N/N	N/N	N/N	N/N	N/N	A/A	N/N	A/A
23	L	1	2	✓	–	✓	N/N	N/N	N/N	N/N	N/N	A/A	N/N	N/N
24	R	1	2	✓	–	✓	N/N	N/N	N/N	N/N	N/N	A/A	N/N	N/N
25	R	1	3	✓	✓	✓	N/N	N/A	N/N	N/A	N/N	A/A	N/N	A/A
26	L	1	3	✓	–	✓	N/N	N/N	N/N	A/A	N/N	A/A	N/N	A/A
27	L	1	3	✓	✓	✓	N/N	A/A	N/N	N/N	N/N	A/A	N/N	A/A
28	R	2	2	–	–	–	N/N	N/N	N/N	N/N	A/A	A/A	N/N	A/A
29	R	2	2	✓	✓	✓	N/N	N/N	N/N	N/N	N/N	A/A	A/A	A/A
30	L	2	2	–	–	–	N/N	N/N	N/N	N/N	A/A	A/A	N/N	A/A
31	L	2	2	–	–	–	N/N	N/N	N/N	N/N	A/A	A/A	A/A	A/A
32	R	2	2	–	–	–	NA/NA	N/N	N/N	N/N	A/A	A/A	A/A	A/A
33	L	2	2	✓	–	✓	N/N	N/N	N/N	N/N	A/A	A/A	NA/NA	A/A
34	R	2	2	–	–	–	N/N	N/N	N/N	N/N	A/A	A/A	A/A	A/A
35	R	2	2	–	–	–	N/N	N/N	N/N	N/N	A/A	A/A	A/A	A/A
36	L	2	2	✓	✓	–	N/N	N/N	N/N	N/N	A/A	A/A	A/A	A/A

Continued on next page

SUPPLEMENTAL TABLE 3. Primer Sequences and Annealing Temperatures for *ABCA4* Gene Screening

Primer	Sequence (5'–3')	Annealing Temperature (C)
Exon 2 forward	GTGTCTGCTCTGGTTACGTTTTC	61
Exon 2 reverse	CCTTTTGTCTAGAAAGATCTTGGG	
Exon 5 forward	TCCAATCGACTCTGGCTGTT	64
Exon 5 reverse	AGAGATCATGGGGCACAACC	
Exon 9 forward	CCAGCATGGAGTTGAATGAGAC	63
Exon 9 reverse	TAAGTGGACTCTTGCGTTTCCTC	
Exon 10 forward	TTAGATTCTGTCAGCCCAGGAAG	63
Exon 10 reverse	ACCAAGTGGGGTCACTGACTTT	
Exon 15 forward	AGAGAGCCCTTTAGGGCAGAAT	63
Exon 15 reverse	GTTTCCTTGGAAGGGTCCGTAG	
Exon 17 forward	AACTGCGGTAAGGTAGGATAGGG	63
Exon 17 reverse	GACCACCTTTCACAAGTTGCTG	
Exon 30 forward	GCCTAGGGATTTGTCAGCAACT	63
Exon 30 reverse	ACTAAACCAAACTCCCTGCACC	
Exon 38 forward	CCAGTTCACACACATCACCTCAG	63
Exon 38 reverse	ATGAGTGCCACTTTCTTCCTCC	
Exon 39 forward	GTGCTGTCCTGTGAGAGCATCTG	64
Exon 39 reverse	GAGGATTAGGGTGCCTCTGTTTC	
Exon 43 forward	CCCGTGTCAACTGGGACTTAG	63
Exon 43 reverse	ATAGTAGGGTGGCTCTGAGGCC	
Exon 44 forward	GCATTTCTGAAGCCAAATAGGAGA	63
Exon 44 reverse	GTGCATTCTCTTGGAGATGAGAAA	
Exon 46-47 forward	TCTTTACTCTTGGATCCACCTCCT	63
Exon 46-47 reverse	GTGTTCTCCATTGACACTTGGAAG	

SUPPLEMENTAL TABLE 2. Normal Ranges for Full-field Electroretinography in Older Adults

	Dark-Adapted 0.01		Dark-Adapted 11.0				Light-Adapted 30 Hz		Light-Adapted 3.0			
			A-wave		B-wave				A-wave		B-wave	
	Amplitude	Peak Time	Amplitude	Peak Time	Amplitude	Peak Time	Amplitude	Peak Time	Amplitude	Peak Time	Amplitude	Peak Time
Age group (≥50 years old)	30-320	76-117	105-495	10-16	235-665	36-57	50-145	22-29	15-60	12-16	90-220	25-32

Dark-adapted 0.01 = dark-adapted dim flash electroretinogram with flash intensity 0.01 candela second (cd·s)/m^2; Dark-adapted 11.0 = dark-adapted bright flash electroretinogram with flash intensity 11.0 cd·s/m^2; Light-adapted 30 Hz = light-adapted 30 Hz flicker electroretinogram with flash intensity 3.0 cd·s/m^2; Light-adapted 3.0 = light-adapted 2 Hz electroretinogram with flash intensity 3.0 cd·s/m^2.

SUPPLEMENTAL TABLE 1. Normal Ranges for Each Component of International Standard Full-field Electroretinography in Young Adults

	Dark-Adapted 0.01		Dark-Adapted 11.0				Light-Adapted 30 Hz		Light-Adapted 3.0			
			A-wave		B-wave				A-wave		B-wave	
	Amplitude (μV)	Peak Time (ms)	Amplitude (μV)	Peak Time (ms)	Amplitude (μV)	Peak Time (ms)	Amplitude (μV)	Peak Time (ms)	Amplitude (μV)	Peak Time (ms)	Amplitude (μV)	Peak Time (ms)
Age group (<50 years old)	135-455	84-107	250-470	7-14	320-755	39-56	70-200	23-27	30-80	12-15	95-295	27-32

Dark-adapted 0.01 = dark-adapted dim flash electroretinogram with flash intensity 0.01 candela second (cd·s)/m^2; Dark-adapted 11.0 = dark-adapted bright flash electroretinogram with flash intensity 11.0 cd·s/m^2; Light-adapted 30 Hz = light-adapted 30 Hz flicker electroretinogram with flash intensity 3.0 cd·s/m^2; Light-adapted 3.0 = light-adapted 2 Hz electroretinogram with flash intensity 3.0 cd·s/m^2.

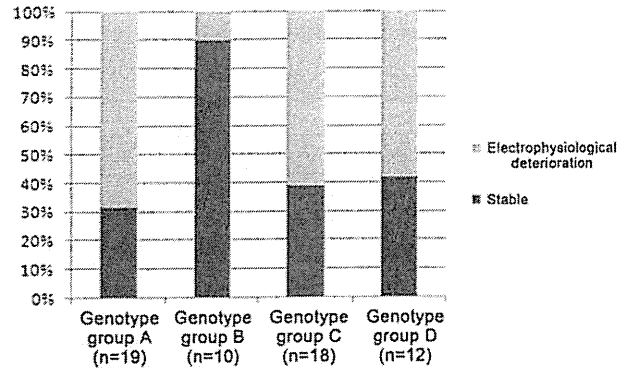

SUPPLEMENTAL FIGURE 2. The association between genotype group and presence or absence of clinically significant electrophysiologic deterioration, showing that patients with Stargardt disease harboring 2 or more non-null variants (genotype group B) more frequently have stable electrophysiologic function over time compared with those with more severe mutations (genotype group A).

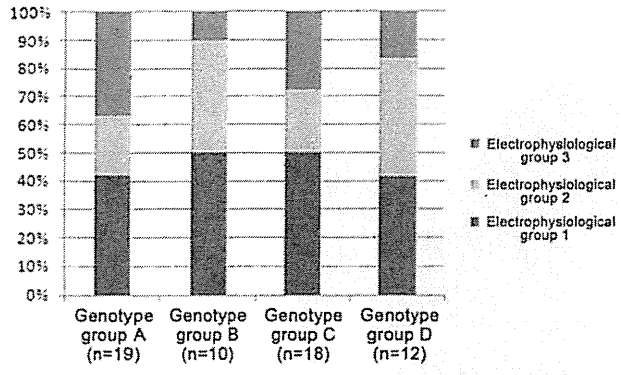

SUPPLEMENTAL FIGURE 1. The association between genotype group and electrophysiologic group at baseline in 59 patients with Stargardt disease, showing that patients with 2 or more null variants (genotype group A) more frequently had generalized rod involvement (electrophysiologic group 3).

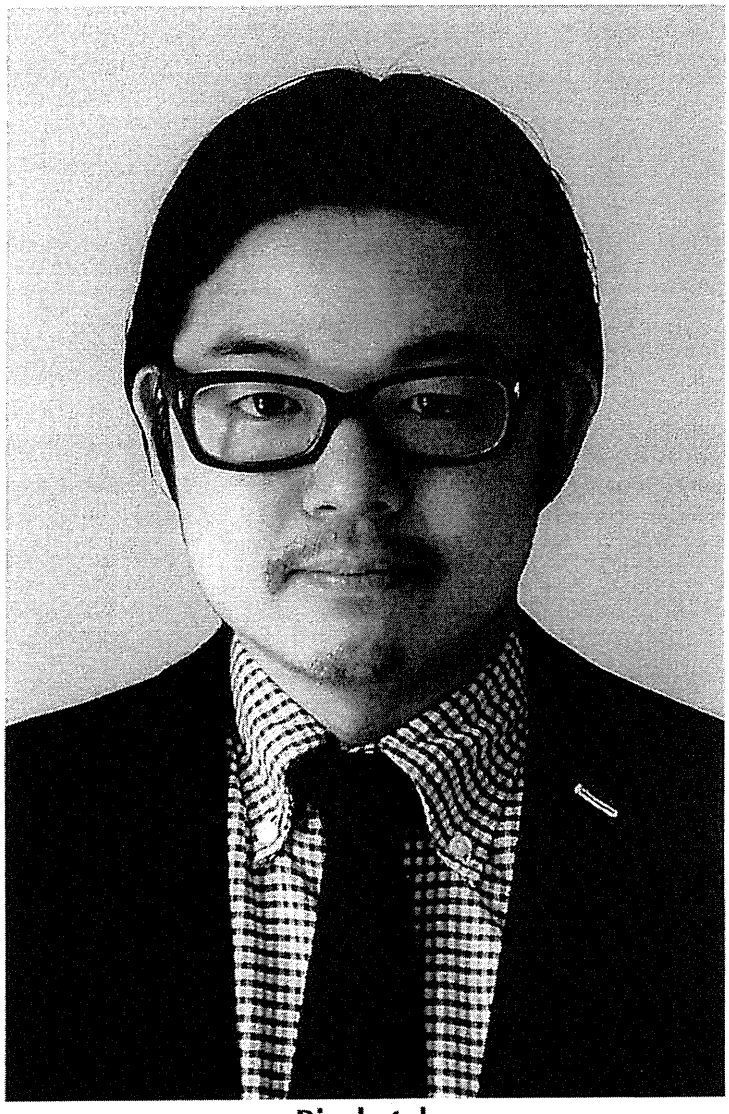

Biosketch

Kaoru Fujinami, MD, is a clinical research fellow in the Departments of Inherited Eye Disease at Moorfields Eye Hospital and Genetics at University College London, Institute of Ophthalmology, United Kingdom. He graduated from Nagoya University and completed ophthalmology clinical training under Professor Miyake at the National Institute of Sensory Organs, Tokyo, Japan. His research interests include clinical electrophysiology and ophthalmic genetics, with his current projects relating to genotype-phenotype correlations in inherited retinal disease.

23. Jaakson K, Zernant J, Kulm M, et al. Genotyping microarray (gene chip) for the ABCR (ABCA4) gene. *Hum Mutat* 2003; 22(5):395–403.
24. Klevering BJ, Blankenagel A, Maugeri A, Cremers FP, Hoyng CB, Rohrschneider K. Phenotypic spectrum of autosomal recessive cone-rod dystrophies caused by mutations in the ABCA4 (ABCR) gene. *Invest Ophthalmol Vis Sci* 2002;43(6):1980–1985.
25. Lewis RA, Shroyer NF, Singh N, et al. Genotype/phenotype analysis of a photoreceptor-specific ATP-binding cassette transporter gene, ABCR, in Stargardt disease. *Am J Hum Genet* 1999;64(2):422–434.
26. Papaioannou M, Ocaka L, Bessant D, et al. An analysis of ABCR mutations in British patients with recessive retinal dystrophies. *Invest Ophthalmol Vis Sci* 2000;41(1):16–19.
27. Rivera A, White K, Stohr H, et al. A comprehensive survey of sequence variation in the ABCA4 (ABCR) gene in Stargardt disease and age-related macular degeneration. *Am J Hum Genet* 2000;67(4):800–813.
28. Rozet JM, Gerber S, Souied E, et al. Spectrum of ABCR gene mutations in autosomal recessive macular dystrophies. *Eur J Hum Genet* 1998;6(3):291–295.
29. Webster AR, Heon E, Lotery AJ, et al. An analysis of allelic variation in the ABCA4 gene. *Invest Ophthalmol Vis Sci* 2001; 42(6):1179–1189.
30. Zernant J, Schubert C, Im KM, et al. Analysis of the ABCA4 gene by next-generation sequencing. *Invest Ophthalmol Vis Sci* 2011;52(11):8479–8487.
31. Lois N, Holder GE, Bunce C, Fitzke FW, Bird AC. Phenotypic subtypes of Stargardt macular dystrophy-fundus flavimaculatus. *Arch Ophthalmol* 2001;119(3):359–369.
32. Holder GE, Brigell MG, Hawlina M, Meigen T. Vaegan, Bach M. ISCEV standard for clinical pattern electroretinography—2007 update. *Doc Ophthalmol* 2007;114(3):111–116.
33. Marmor MF, Fulton AB, Holder GE, Miyake Y, Brigell M, Bach M. ISCEV Standard for full-field clinical electroretinography (2008 update). *Doc Ophthalmol* 2009;118(1):69–77.
34. Robson AG, Webster AR, Michaelides MM, et al. "Cone dystrophy with supernormal rod electroretinogram": a comprehensive genotype/phenotype study including fundus autofluorescence and extensive electrophysiology. *Retina* 2010;30(1):51–62.
35. Lenassi E, Robson AG, Hawlina M, Holder GE. The value of two-field pattern electroretinogram in routine clinical electrophysiologic practice. *Retina* 2012;32(3):589–599.
36. Orita M, Iwahana H, Kanazawa H, Hayashi K, Sekiya T. Detection of polymorphisms of human DNA by gel electrophoresis as single-strand conformation polymorphisms. *Proc Natl Acad Sci U S A* 1989;86(8):2766–2770.
37. Ng PC, Henikoff S. SIFT: predicting amino acid changes that affect protein function. *Nucleic Acids Res* 2003;31(13): 3812–3814.
38. Adzhubei IA, Schmidt S, Peshkin L, et al. A method and server for predicting damaging missense mutations. *Nat Methods* 2010;7(4):248–249.
39. Weleber RG. The effect of age on human cone and rod ganzfeld electroretinograms. *Invest Ophthalmol Vis Sci* 1981;20(3): 392–399.
40. Cella W, Greenstein VC, Zernant-Rajang J, et al. G1961E mutant allele in the Stargardt disease gene ABCA4 causes bull's eye maculopathy. *Exp Eye Res* 2009;89(1):16–24.
41. Martinez-Mir A, Paloma E, Allikmets R, et al. Retinitis pigmentosa caused by a homozygous mutation in the Stargardt disease gene ABCR. *Nat Genet* 1998;18(1):11–12.
42. Schindler EI, Nylen EL, Ko AC, et al. Deducing the pathogenic contribution of recessive ABCA4 alleles in an outbred population. *Hum Mol Genet* 2010;19(19):3693–3701.
43. Simonelli F, Testa F, Zernant J, et al. Genotype-phenotype correlation in Italian families with Stargardt disease. *Ophthalmic Res* 2005;37(3):159–167.
44. Klevering BJ, Yzer S, Rohrschneider K, et al. Microarray-based mutation analysis of the ABCA4 (ABCR) gene in autosomal recessive cone-rod dystrophy and retinitis pigmentosa. *Eur J Hum Genet* 2004;12(12):1024–1032.
45. Maugeri A, van Driel MA, van de Pol DJ, et al. The 2588G–>C mutation in the ABCR gene is a mild frequent founder mutation in the Western European population and allows the classification of ABCR mutations in patients with Stargardt disease. *Am J Hum Genet* 1999;64(4): 1024–1035.

over a 10-year period, compared to 100% of those with an initial rod system ERG abnormality. These data assist the counseling of the patient in relation to visual prognosis and may inform the design, patient selection, and monitoring of current and future clinical trials for *ABCA4*-related retinopathy.

ALL AUTHORS HAVE COMPLETED AND SUBMITTED THE ICMJE FORM FOR DISCLOSURE OF POTENTIAL CONFLICTS OF INTEREST and none were reported. Publication of this article was supported by grants from the National Institute for Health Research Biomedical Research Centre at Moorfields Eye Hospital NHS Foundation Trust and University College London, Institute of Ophthalmology (UK), Fight For Sight (UK), Moorfields Eye Hospital Special Trustees (UK), Macular Disease Society (UK), the Foundation Fighting Blindness (USA), Suzuken Memorial Foundation (Japan), Mitsukoshi Health and Welfare Foundation (Japan), and Daiwa Anglo-Japanese Foundation (Japan). M.M. is supported by an FFB Career Development Award (USA). Contributions of authors: conception and design (K.F., N.L., A.D., A.W., G.H., M.M.); analysis and interpretation (K.F., N.L., A.D., D.M., C.H., E.S., K. Tsunoda., C.B., A.R., A.M., A.W., G.H., M.M.); writing the article (K.F., A.D., A.R., A.W., K. Tsubota., C.B., G.H., M.M.); critical revision of the article (K.F., N.L., A.D., E.S., K.Tsunoda, K.Tsubota, C.B., A.W., G.H., M.M.); final approval of the article (K.F., K. Tsunoda., C.B., A.T., A.W., G.H., M.M.); data collection (K.F., A.D., D.M., C.H., E.S., A.R., A.M., A.W., G.H., M.M.); provision of materials, patients, or resources (K.F., A.R., A.M., A.W., G.H., M.M.); statistical expertise (K.F., K. Tsubota., C.B., M.M.); obtaining funding (K.F., D.M., K. Tsunoda., A.M., A.W., M.M.); literature search (K.F., A.D., D.M., K. Tsunoda., A.R., M.M.); and administrative, technical, or logistic support (K.F., C.H., A.R., M.M.). The authors are grateful to those who contributed to the assembly of the *ABCA4* panel, particularly Naushin Waseem, Bev Scott, Genevieve Wright, Sophie Devery, and Ravinder Chana (University College London, Institute of Ophthalmology, London, United Kingdom). The authors thank Professor Yozo Miyake (Aichi Medical University, Aichi, Japan), Panagiotis Sergouniotis, Rajarshi Mukhopadhyay, Arundhati Dev Borman, Eva Lenassi (University College London, Institute of Ophthalmology, London, United Kingdom), and Jean Andorf (University of Iowa Institute for Vision Research, Howard Hughes Medical Institute, Iowa City, Iowa, USA) for their insightful comments.

REFERENCES

1. Stargardt K. Uber familiare progressive degeneration in der makulagegend des auges. *Albrecht von Graefes Arch Klin Ophthalmol* 1909;71:534–550.
2. Franceschetti A, Francois J. Fundus flavimaculatus. *Arch Ophthalmol* 1965;25(6):505–530.
3. Michaelides M, Hunt DM, Moore AT. The genetics of inherited macular dystrophies. *J Med Genet* 2003;40(9): 641–650.
4. Lois N, Halfyard AS, Bird AC, Holder GE, Fitzke FW. Fundus autofluorescence in Stargardt macular dystrophy-fundus flavimaculatus. *Am J Ophthalmol* 2004;138(1):55–63.
5. McBain VA, Townend J, Lois N. Progression of retinal pigment epithelial atrophy in stargardt disease. *Am J Ophthalmol* 2012;154(1):146–154.
6. Jayasundera T, Rhoades W, Branham K, Niziol LM, Musch DC, Heckenlively JR. Peripapillary dark choroid ring as a helpful diagnostic sign in advanced stargardt disease. *Am J Ophthalmol* 2010;149(4):656–660.
7. Rotenstreich Y, Fishman GA, Anderson RJ. Visual acuity loss and clinical observations in a large series of patients with Stargardt disease. *Ophthalmology* 2003;110(6):1151–1158.
8. von Ruckmann A, Fitzke FW, Bird AC. In vivo fundus autofluorescence in macular dystrophies. *Arch Ophthalmol* 1997; 115(5):609–615.
9. Walia S, Fishman GA. Natural history of phenotypic changes in Stargardt macular dystrophy. *Ophthalmic Genet* 2009;30(2): 63–68.
10. Allikmets R, Singh N, Sun H, et al. A photoreceptor cell-specific ATP-binding transporter gene (ABCR) is mutated in recessive Stargardt macular dystrophy. *Nat Genet* 1997; 15(3):236–246.
11. Allikmets R, Shroyer NF, Singh N, et al. Mutation of the Stargardt disease gene (ABCR) in age-related macular degeneration. *Science* 1997;277(5333):1805–1807.
12. Burke TR, Tsang SH. Allelic and phenotypic heterogeneity in ABCA4 mutations. *Ophthalmic Genet* 2011;32(3): 162–174.
13. Cremers FP, van de Pol DJ, van Driel M, et al. Autosomal recessive retinitis pigmentosa and cone-rod dystrophy caused by splice site mutations in the Stargardt's disease gene ABCR. *Hum Mol Genet* 1998;7(3):355–362.
14. Fishman GA, Stone EM, Eliason DA, Taylor CM, Lindeman M, Derlacki DJ. ABCA4 gene sequence variations in patients with autosomal recessive cone-rod dystrophy. *Arch Ophthalmol* 2003;121(6):851–855.
15. Klevering BJ, Deutman AF, Maugeri A, Cremers FP, Hoyng CB. The spectrum of retinal phenotypes caused by mutations in the ABCA4 gene. *Graefes Arch Clin Exp Ophthalmol* 2005;243(2):90–100.
16. Lois N, Holder GE, Fitzke FW, Plant C, Bird AC. Intrafamilial variation of phenotype in Stargardt macular dystrophy-Fundus flavimaculatus. *Invest Ophthalmol Vis Sci* 1999; 40(11):2668–2675.
17. Michaelides M, Chen LL, Brantley MA Jr, et al. ABCA4 mutations and discordant ABCA4 alleles in patients and siblings with bull's-eye maculopathy. *Br J Ophthalmol* 2007; 91(12):1650–1655.
18. van Driel MA, Maugeri A, Klevering BJ, Hoyng CB, Cremers FP. ABCR unites what ophthalmologists divide(s). *Ophthalmic Genet* 1998;19(3):117–122.
19. Fujinami K, Akahori M, Fukui M, Tsunoda K, Iwata T, Miyake Y. Stargardt disease with preserved central vision: identification of a putative novel mutation in ATP-binding cassette transporter gene. *Acta Ophthalmol* 2011;89(3):e297–e298.
20. Briggs CE, Rucinski D, Rosenfeld PJ, Hirose T, Berson EL, Dryja TP. Mutations in ABCR (ABCA4) in patients with Stargardt macular degeneration or cone-rod degeneration. *Invest Ophthalmol Vis Sci* 2001;42(10):2229–2236.
21. Fishman GA, Stone EM, Grover S, Derlacki DJ, Haines HL, Hockey RR. Variation of clinical expression in patients with Stargardt dystrophy and sequence variations in the ABCR gene. *Arch Ophthalmol* 1999;117(4):504–510.
22. Fumagalli A, Ferrari M, Soriani N, et al. Mutational scanning of the ABCR gene with double-gradient denaturing-gradient gel electrophoresis (DG-DGGE) in Italian Stargardt disease patients. *Hum Genet* 2001;109(3):326–338.

electrophysiologic deterioration. The 3 patients who progressed from Group 1 to Group 2 had abnormal light-adapted 30 Hz ERGs without any abnormalities in light-adapted 3.0 ERGs; the 30 Hz flicker ERG is known to be a more sensitive indicator of altered cone function than the single-flash photopic ERG. In contrast, both cone full-field ERGs were abnormal in the 3 patients who progressed from Group 1 to Group 3. All 6 patients had a >3 ms peak time shift over time; careful observation of the light-adapted 30 Hz ERGs is important in monitoring Stargardt disease patients with normal ERGs. All but 1 patient with abnormalities in dark-adapted 0.01 or dark-adapted 11.0 had abnormal cone responses, suggesting that generalized cone system dysfunction precedes generalized rod system dysfunction, as has previously been demonstrated.[31]

All 5 patients with undetectable cone responses at follow-up had a >50% amplitude reduction in dark-adapted 11.0 during follow-up. Four patients still had residual responses in dark-adapted 11.0 at follow-up and 1 patient had residual responses in dark-adapted 11.0 at baseline, which became undetectable at follow-up. These findings lend further support to the belief that generalized cone system function is abolished before generalized rod system loss, and that the amplitude of dark-adapted 11.0 responses may be helpful in assessing residual retinal function in cases with very severe retinal dysfunction.

The clinical characteristics of each ERG group showed a statistically significant difference between Groups 1 and 3 and Groups 2 and 3 in terms of age of onset, in keeping with the original cross-sectional data, with a younger age of onset associated with more generalized retinal dysfunction.[31] There was also a statistically significant difference in logMAR VA between Groups 1 and 3 and Groups 2 and 3, with worse VA associated with increasingly severe generalized retinal dysfunction, as has been previously proposed.[31] No statistically significant differences were observed between groups with respect to other parameters, including age at baseline, duration of disease, and interval of follow-up. In addition, the age of onset was earlier in subjects who had clinically significant ERG progression compared to those who did not meet criteria for clinically significant deterioration, further supporting the likelihood that age of onset in Stargardt disease is of prognostic value.[7] For ease of comparison between groups, a linear longitudinal relationship has been assumed and the rate of change expressed in terms of yearly amplitude reduction, yearly percentage reduction, and yearly peak time shift. This study has not examined the linearity of change between baseline and follow-up testing; a prospective study with additional, more frequent time point sampling will help address this pertinent question. It is likely that progression will be linear in some individuals and nonlinear in others, in keeping with the commonplace phenotypic heterogeneity of inherited retinal disorders.

ABCA4 mutations were originally reported in patients with autosomal recessive Stargardt disease but shortly thereafter were identified in association with cone dystrophy, cone-rod dystrophy, and "retinitis pigmentosa," with a genotype-phenotype relationship having been proposed.[10,13–15,21,24,40–43] In the present cohort, 82% of patients (22/27) in ERG Group 1 at baseline, 70% (12/17) in Group 2, and 87% (13/15) in Group 3 harbored at least 1 *ABCA4* variant.

A likely disease-causing *ABCA4* variant was identified in 47 out of 59 patients, with 6 putative novel mutations detected. There was no statistically significant association identified between the category of genotype and the extent of electrophysiologic dysfunction on the basis of ERG group, although patients with 2 or more non-null variants (genotype B group) less frequently had rod ERG involvement. A statistically significant greater percentage of patients with null variants (genotype A group) (68%, 13/19) had ERG deterioration, in comparison with patients harboring 2 or more non-null variants (10%, 1/10), with the majority therefore having a stable ERG (90%, 9/10). There was also a statistically significant difference between genotype groups A and B with respect to yearly amplitude reduction of dark-adapted 11.0 a-wave and light-adapted 30 Hz yearly peak time shift. There are several factors that may account for the relative lack of more clearly demonstrable genotype-phenotype correlations, including the relatively small sample size, the fact that only 1 disease-causing allele was identified in most cases, and the vast allelic heterogeneity of *ABCA4*. However, one particular variant (c.5461-10T>C) was found to be associated with electrophysiologic progression. This mutation has been previously reported to be associated with severe disease in both the homozygous and compound heterozygous states,[42,44] suggesting that it may be a marker for more severe disease, which is likely to show clinically significant progression.

Co-inheritance of p.Arg943Gln and p.Gly863Ala has been previously reported,[44,45] with p.Arg943Gln thought to be a benign polymorphism[29,45] and p.Gly863Ala believed to be associated with milder phenotypes,[42,45] although there has been a single report of a severe phenotype associated with p.Gly863Ala in the homozygous configuration.[44] Only 2 out of 8 patients harboring p.Gly863Ala in the present series had evidence of ERG progression, suggesting this variant is indeed likely to be associated with milder disease.

The longitudinal study described herein has identified that a patient's allocation to an individual ERG group, as proposed in the original cross-sectional study, may change over time—a conclusion that could not be made previously because of the inherent limitations of a cross-sectional survey. The rate of progression between groups and within groups has been determined, and age of onset and, to a lesser extent, visual acuity may predict the degree of eventual generalized retinal dysfunction and/or progression. It is important that only 20% of those patients with initially normal full-field ERGs showed evidence of progression

TABLE 4. Yearly Change[a] in Dark-Adapted Bright Flash Electrophysiologic Responses and Light-Adapted 30 Hz Flicker Responses With Respect to Electrophysiologic Group at Baseline, Electrophysiologic Deterioration, and Genotype Group, in 59 Subjects With Stargardt Disease

	Dark-Adapted 11.0 A-wave			Light-Adapted 30 Hz		
	Amplitude Reduction (μV/y)	Percentage Reduction (%/y)	Peak Time Shift (ms/y)	Amplitude Reduction (μV/y)	Percentage Reduction (%/y)	Peak Time Shift (ms/y)
Group 1 (n = 27)	5.5	1.7	0.10	2.7	2.2	0.14
Group 2 (n = 17)	4.5	1.5	0.09	1.1	1.7	0.19
Group 3 (n = 15)	4.9	3.6	0.18	1.5	3.1	0.32
Stable (n = 27)	3.9	1.2	0.04	2.2	1.9	0.07
Electrophysiologic Deterioration (n = 32)	6.0	2.9	0.18	1.7	2.7	0.31
Genotype A (n = 19)	6.5	3.0	0.14	2.3	3.0	0.23
Genotype B (n = 10)	2.3	0.5	−0.01	1.4	0.9	0.12
Genotype C (n = 18)	5.4	2.1	0.16	2.4	3.1	0.33
Genotype D (n = 12)	4.3	2.1	0.09	1.1	0.9	−0.04
Total (n = 59)	5.1	2.1	0.11	1.9	2.3	0.19

Dark-adapted 11.0 = dark-adapted bright flash electroretinogram (flash intensity 11.0 candela seconds (cd·s)/m^2); Light-adapted 30 Hz = light-adapted 30 Hz flicker electroretinogram (flash intensity 3.0 cd·s/m^2).

[a]A yearly amplitude reduction and a yearly percentage reduction were calculated by dividing the amplitude reduction or the percentage reduction by the follow-up time. A yearly peak time shift (difference between peak time at baseline and follow-up) was also calculated by dividing by the follow-up time.

TABLE 5. Distribution of the 4 Genotype Groups With Respect to Electrophysiologic Group at Baseline and Electrophysiologic Deterioration in Stargardt Disease

	Genotype A	Genotype B	Genotype C	Genotype D
Group 1 (n = 27)	8	5	9	5
Group 2 (n = 17)	4	4	4	5
Group 3 (n = 15)	7	1	5	2
Stable (n = 27)	6	9	7	5
Electrophysiologic deterioration (n = 32)[a]	13	1	11	7
Total (n = 59)	19	10	18	12

[a]The subset without evidence of significant deterioration is described as "Stable."

shown in Table 5 and Supplemental Figure 2 (available at AJO.com). Statistical analysis revealed a significant difference between genotype groups A and B and between genotype groups A and C in terms of age of onset. There was also a statistically significant difference between genotype groups A and B with respect to yearly amplitude reduction of dark-adapted 11.0 a-wave and light-adapted 30 Hz yearly peak time shift (Supplemental Table 5). No statistically significant difference was seen between genotype groups and the other ERG parameters (Supplemental Table 5).

Interestingly, 8 of the 9 patients harboring the variant c.5461-10 T>C (Patients 5, 25, 36, 39, 48, 50, 53-55) had clinically significant ERG progression. All 3 unrelated patients (1, 5, and 31) harboring p.Arg943Gln also had p.Gly863Ala, suggesting linkage disequilibrium of these 2 substitutions, with none of these subjects having clinically significant ERG deterioration.

DISCUSSION

THIS REPORT ADDRESSES LONGITUDINAL CHANGES IN CLINical and electrophysiologic features of Stargardt disease in a large, well-characterized cohort of patients, with 1 or both likely disease-causing *ABCA4* alleles identified in 80% of subjects (47/59). The findings confirm the prognostic value of ERG suggested by earlier cross-sectional data and are relevant to the design of future clinical trials.

Approximately one-fifth of Group 1 patients (dysfunction confined to the macula) progressed to either Group 2 or Group 3 (generalized retinal dysfunction) over a mean time period of 10.5 years, whereas 47% of subjects with Group 2 ERG at baseline changed to Group 3 over the same time period. Overall, there was clinically significant electrophysiologic deterioration in 54% of all patients (32/59), with progression in 22% (6/27) of Group 1 subjects, 65% (11/17) of Group 2, and 100% (15/15) of Group 3. These ERG changes far exceed estimates of normal age-related ERG decline.[39] Thus all patients with initial rod involvement (Group 3) demonstrated clinically significant electrophysiologic deterioration, but only 22% of the patients with normal ERGs (Group 1) at baseline showed clinically significant progression.

A transition in ERG group was seen in 14 patients, with all 14 also meeting the criteria for clinically significant